Book: Holistic Simulation of Geotechnical Installation Processes
Year: 2016

Constitutive Model for Clays Under the ISA Framework

W. Fuentes, M. Hadzibeti and Theodoros Triantafyllidis

Abstract The Intergranular Strain Anisotropy ISA framework is a novel approach to develop elastoplastic models wherein a yield surface is defined in terms of strain increments. For this purpose, the loading-unloading conditions are satisfied within the space of the intergranular strain, this latter being a state variable "following" the strain rate. With this, the model aims to improve the simulations under cyclic loading while keeping their good capabilities at monotonic loading. Within this article, a constitutive model for clays is developed under the ISA plasticity framework. The model adopts some parameters from the modified Cam-Clay model and others to describe the evolution of the integranular strain and its effect on the model response. Some illustrative simulations are provided to analyze the model performance under cyclic loading. The simulations show a qualitative behavior in agreement with some experiments. Possible improvements are discussed at the end of the article.

Keywords Clay model · ISA plasticity · Intergranular strain

1 Introduction

The intergranular strain anisotropy (ISA) plasticity, recently proposed by Fuentes and Triantafyllidis [4], is a mathematical framework useful for the development of constitutive models simulating the cyclic behavior of the material. It is based on the concept of the intergranular strain [11], being a state variable which provides information about the recent strain history. Specifically, the intergranular strain variable has information related with the change of strain rate direction $\overrightarrow{\dot{\epsilon}}$ within a strain amplitude of approximately $|| \Delta\varepsilon || \approx 10^{-3}$. Having this, the constitutive model increases the stiffness and reduces the plastic accumulation upon every change of strain rate direction $\overrightarrow{\dot{\epsilon}}$. All these effects have shown to provide a better performance of the simulations under cyclic loading.

The idea of the intergranular strain was originally proposed by Niemunis and Herle [11] in order to mitigate the excessive plastic accumulation exhibited by some Karlsruhe hypoplastic models, e.g., the model by [13]. The physical explanation attributed to this variable, even this is debatable, consists in the idea that it represents the deformations of the interface layers between the soil particles (intergranular space) and accordingly, very small deformations of these interfaces are responsible of the small strain effects, namely the stiffness increase, the reduction of the plastic strain rate, and the appearance of an elastic locus upon cyclic loading. The formulation by Niemunis and Herle [11] did simulate well some of aforementioned small strain effects except for the appearance of an elastic locus, fact which motivated the development of the recently proposed ISA formulation [3], in which an elastic locus of the material within the space of the intergranular strain and other small strain effects are truly considered.

So far with the new ISA framework, the formulation has shown to simulate well tests performing cyclic loading on sands [3, 4], but still not been tested on the simulations of fine-grained soils. Therefore, this article is committed to show the performance of the model with a direct focus on the simulation of the clay mechanical behavior. The relations presented herein are mostly based on the previous model for sands by Fuentes and Triantafyllidis [4] but modified to account for additional required effects of clays. While the evolution equation of the intergranular strain remains identical as in the previous formulation [4], some other relations have been modified for the sake of convenience, namely the compression law at isotropic conditions, the dilatancy surface which now coincides with the critical state surface and an overconsolidation factor considered to improve the simulations under these states. The details of the new relations will be provided in the next sections.

The notation of this article is as follows. Scalar quantities are denoted with italic fonts (e.g., a, b), second rank tensors with bold fonts (e.g., $\mathbf{A}$, $\boldsymbol{\sigma}$), and fourth rank tensors with Sans Serif type (e.g., E, L). Multiplication with two dummy indices, also known as double contraction, is denoted with a colon ":" (e.g., $\mathbf{A} : \mathbf{B} = A_{ij} B_{ij}$). When the symbol is omitted, it is then interpreted as a dyadic product (e.g., $\mathbf{AB} = A_{ij} B_{kl}$). The deviatoric component of a tensor is symbolized with an asterisk as superscript $\mathbf{A}^*$. The effective stress tensor is denoted with $\boldsymbol{\sigma}$ and the strain tensor with ε. The Roscoe invariants are defined as $p = -\mathrm{tr}\boldsymbol{\sigma}/3$, $q = \sqrt{3/2} \parallel \boldsymbol{\sigma}^* \parallel$, $\varepsilon_v = -\mathrm{tr}\boldsymbol{\epsilon}$ and $\varepsilon_s = \sqrt{2/3} \parallel \boldsymbol{\epsilon}^* \parallel$.

2 Intergranular Strain Model

Conventionally, constitutive models for soils propose yield functions describing a surface within the stress space. In Contrast to this, the ISA plasticity focuses on the incorporation of the elastic locus in terms of strain amplitudes (within the strain space) and not within the stress space. A yield function with such characteristics is expected to depend on a variable having information of the strain amplitude. One of the simplest idea to compute the current strain amplitude would be to subtract

from the current strain the one at the last reversal point, as by the paraelastic models [12]. Nevertheless, this operation may be numerically unstable when dealing with very small strain amplitudes $|| \varepsilon || < 10^{-4}$. On the contrary, the intergranular strain does not need the introduction of reversal points, but gives information about the strain amplitude. In the following lines, the formulation of the intergranular strain according to the ISA model is recalled [4].

Consider an elastic locus of the material within the intergranular strain space $\mathbf{h}$, described with a yield function $F_H = F_H(\mathbf{h}, \mathbf{c}) = 0$ whereby $\mathbf{c}$ is a hardening variable to be defined in the sequel. It is now established that if $F_H < 0$, the response of the material is elastic, and the intergranular strain $\mathbf{h}$ evolves identically as the strain ε does:

$$\dot{\mathbf{h}} = \dot{\epsilon} \qquad \text{for} \qquad F_H < 0 \tag{1}$$

This is a very convenient evolution equation, since any hardening variable (as the yet unknown tensor $\mathbf{c}$) remains constant under elastic conditions $F_H < 0$, and the increments of intergranular strain are equal to the increments of strain, i.e., $\Delta\mathbf{h} = \Delta\varepsilon$. This latter condition is very useful to define a yield function describing an elastic locus in terms of strain amplitude. If the strain amplitude of the elastic locus is constant, this surface looks like a sphere within the principal intergranular strain space whose center is represented with $\mathbf{c}$. Following this, the yield function can be defined as:

$$\text{IS yield surface:} \qquad F_H \equiv \| \mathbf{h} - \mathbf{c} \| - R/2 = 0 \tag{2}$$

whereby the tensor $\mathbf{c}$ has been termed the "back-intergranular strain" being actually a hardening variable, and the parameter R is a constant representing the maximum amplitude of the elastic strains. In the space of the volumetric invariant $h_v/\sqrt{3} = -\text{tr}(\mathbf{h})/\sqrt{3}$ and the deviator invariant $\sqrt{3/2}h_s = \| \mathbf{h}^* \|$, where $\mathbf{h}^*$ is the deviator intergranular strain, the IS yield surface from Eq. 2 takes exactly the form of a circle, as illustrated in Fig. 1.

Now consider the plastic case in which the intergranular strain "touches" the yield surface $F_H = F_H(\mathbf{h}, \mathbf{c}) = 0$. In that case, it is desired that after a reversal loading, the material exhibits smoothly the appearance of a plastic strain rate. Brittle materials would present a very rapid change of the stiffness when changing from elastic to plastic behavior, but most soils and some other materials show actually a smooth stiffness transition when it turns from the elastic into plastic regime. This effect can be well simulated through a hardening mechanism of the yield surface described with tensor $\mathbf{c}$. For the ISA framework, some simple relations of the bounding surface plasticity have been adopted to simulate this behavior. Hence, the model considers besides the yield surface a bounding surface within the intergranular strain space.

To formulate the behavior under plastic conditions $F_H = 0$, a plastic term is added to the intergranular strain evolution equation:

$$\dot{\mathbf{h}} = \dot{\epsilon} - \dot{\lambda}_H \mathbf{N} \qquad \text{for} \qquad F_H = 0 \tag{3}$$

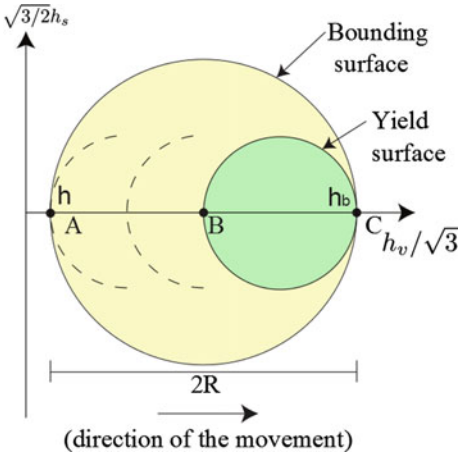

Fig. 1 Yield surface and bounding surface within the space of the intergranular strain

whereby $\dot{\lambda}_H$ is a consistency parameter and $\mathbf{N}$ is the intergranular strain flow rule being normal to the IS yield surface (see Fig. 1):

$$\mathbf{N} = (\mathbf{h} - \mathbf{c})^{\rightarrow} \tag{4}$$

In the last equation, the operator $\sqcup^{\rightarrow}$ extracts the direction of the tensor $\sqcup^{\rightarrow} = \sqcup / \parallel \sqcup \parallel$. The consistency parameter $\dot{\lambda}_H \geq 0$ in Eq. 3 is related with the yield surface function F_H and deduced considering the consistency condition $\dot{F}_H = 0$.

The bounding surface within the intergranular strain space is depicted in Fig. 1. This surface has the same shape as the yield surface but with twice its size and a center at the origin. Its function takes the following form:

$$\text{IS bounding surface:} \qquad F_{Hb} \equiv \parallel \mathbf{h} \parallel - R = 0 \tag{5}$$

The evolution equation for the back-intergranular strain $\mathbf{c}$ can be expressed as a function of the consistency parameter $\dot{\lambda}_H$:

$$\dot{\mathbf{c}} = \dot{\lambda}_H \bar{\mathbf{c}} \tag{6}$$

whereby $\bar{\mathbf{c}}$ is its hardening function. The hardening function $\bar{\mathbf{c}}$ presents the following relation:

$$\bar{\mathbf{c}} = \beta(\mathbf{c}_b - \mathbf{c})/R \qquad \text{with} \qquad \mathbf{c}_b = R/2(\dot{\boldsymbol{\epsilon}})^{\rightarrow} \tag{7}$$

whereby β is a material parameter and $\mathbf{c}_b$ is the image of $\mathbf{c}$ at the bounding surface. The consistency condition $\dot{F}_H = 0$ followed by substitution with Eqs. 2, 6, 7 and 3 yields to the consistency parameter definition $\dot{\lambda}_H$:

$$\dot{\lambda}_H = \frac{\langle \mathbf{N} : \dot{\boldsymbol{\epsilon}} \rangle}{1 + H_H} \tag{8}$$

where the operator $\langle\rangle$ are the Macaulay brackets and $H_H = -(\partial F_H/\partial \mathbf{c}) : \bar{\mathbf{c}}$ is the hardening modulus.

In the following lines, a scalar function is introduced to quantify how close is the intergranular strain $\mathbf{h}$ to the bounding surface $F_{Hb} = 0$. Similar to the image tensor $\mathbf{c}_b$, one can propose an image tensor of the intergranular strain at the bounding surface denoted by $\mathbf{h}_b$ and defined as:

$$\mathbf{h}_b = R\mathbf{N} \tag{9}$$

The distance $\| \mathbf{h}_b - \mathbf{h} \|$ provides information of how close is the intergranular strain $\mathbf{h}$ to the bounding surface $F_{Hb} = 0$. According to the proposed model, the bounding condition $\mathbf{h} = \mathbf{h}_b$ should be asymptotically reached after applying large strains in a constant direction $\overrightarrow{\dot{\epsilon}}$. At these states, $\mathbf{N}$ should reach the value of $\overrightarrow{\dot{\epsilon}}$. This particular state in which $\mathbf{N} = \overrightarrow{\dot{\epsilon}}$ and $\mathbf{h} = R\overrightarrow{\dot{\epsilon}}$ has been called the "fully mobilized" state. The scalar function ρ is introduced to consider how close is the current state to this "fully mobilized" state:

$$\rho = 1 - \frac{\| \mathbf{h}_b - \mathbf{h} \|}{2R} \tag{10}$$

This scalar function provides two important and illustrative cases. It renders $\rho = 0$ when $\| \mathbf{h}_b - \mathbf{h} \| = 2R$, which means strain reversal after fully mobilized state. On the other side, $\rho = 1$ when $\mathbf{h} = \mathbf{h}_b$ for fully mobilized state. The last case is very useful when formulating relations of the mechanical model under medium and large strain amplitudes.

3 Mechanical Model Formulation

Having defined the evolution equation of the intergranular strain $\mathbf{h}$, it is now proceeded with the description of the mechanical model which relates the rate of (effective) stress $\dot{\boldsymbol{\sigma}}$ with the rate of the strain $\dot{\epsilon}$. The constitutive relation is based on the ISA plasticity framework [3] which can be written with the following general form:

$$\dot{\boldsymbol{\sigma}} = m\bar{\mathbf{E}} : (\dot{\boldsymbol{\epsilon}} - y_h \bar{\dot{\boldsymbol{\epsilon}}}^p) \tag{11}$$

where $\bar{\mathbf{E}}$ is the residual stiffness, or with other words, the stiffness at mobilized states $\rho = 1$, the tensor $\bar{\dot{\boldsymbol{\epsilon}}}^p$ corresponds to the plastic strain rate at mobilized states $\rho = 1$ and the scalar functions m and y_h have been introduced to increase the stiffness and reduce the plastic strain rate, respectively, upon cyclic loading ($y_h < 1$). The factor y_h is proposed, such that it reduces the plastic strain rate upon unloading and guarantees the stress rate continuity between the elastic and plastic response. The simulation of these two effects are achieved through the multiplication of two factos as follows:

$$y_h = \rho^{\chi_h} \langle \mathbf{N} : \overrightarrow{\dot{\boldsymbol{\epsilon}}} \rangle \tag{12}$$

whereby the factor ρ^{χ_h} reduces the plastic strain rate upon cyclic loading and the factor $\langle \mathbf{N} : \dot{\boldsymbol{\epsilon}} \rangle$ is the one responsible of the stress rate continuity. Notice that this factor also appears in the numerator of the consistency parameter Eq. 8, fact which is not a coincidence. Notice also that when $y_h = 0$, the response is (hypo-)elastic whereas $y_h = 1$ implies fully mobilized states.

The factor m responsible for the stiffness increase is a simple function interpolating between $1 \leq m \leq m_R$, whereby $m_R > 1$ is a material constant. The function from Fuentes and Triantafyllidis [4] is here adopted:

$$m = m_R + (1 - m_R) y_h \tag{13}$$

One of the main features of the ISA plasticity is that at fully mobilized states, the effect of the scalar functions m and y_h vanishes, i.e., $m = 1$ and $y_h = 1$, and the general constitutive equation yields to:

$$\begin{aligned} \dot{\boldsymbol{\sigma}} &= \bar{\mathsf{E}} : (\dot{\boldsymbol{\epsilon}} - \bar{\dot{\boldsymbol{\epsilon}}}^p) \\ &= \bar{\mathsf{E}} : (\dot{\boldsymbol{\epsilon}} - Y \mathbf{m} \parallel \dot{\boldsymbol{\epsilon}} \parallel) \end{aligned} \tag{14}$$

whereby $Y = \parallel \bar{\dot{\boldsymbol{\epsilon}}}^p \parallel / \parallel \dot{\boldsymbol{\epsilon}} \parallel$ is the degree of nonlinearity [10] and $\mathbf{m} = \overrightarrow{\bar{\dot{\boldsymbol{\epsilon}}}^p}$ is a flow rule ($\parallel \mathbf{m} \parallel = 1$). This particular form can be adjusted to the mechanical behavior exhibited by the material at medium and large strain amplitudes at which the condition $y_h = 1$ is expected. Furthermore, it recalls some constitutive equations proposed in the literature, whereby a plastic strain component is always active, such as the Karlsruhe hypoplastic models [6, 10, 13], which according to some authors, simulate well the behavior at these strain amplitudes. Hence, even this is not a must, one may adopt some existing formulations of the Karlsurhe hypoplastic model for the tensors $\bar{\mathsf{E}}$ and $\bar{\dot{\boldsymbol{\epsilon}}}^p$. To give an example, if the interest focuses on the simulation of the behavior of clays, it is possible to adopt directly the existing relations for $\bar{\mathsf{E}}$ and $\bar{\dot{\boldsymbol{\epsilon}}}^p$ from the hypoplastic model by Masin [9]. Anyway, within this work a similar formulation as the previous ISA-type model for sands by [4] is adopted as reference, and some of its functions are modified to simulate the clay behavior. These modifications are based on some conventional concepts, such as the distinction of normal consolidated and overconsolidated states which are explained within the next sections. Further steps toward the model development are still missing, such as the consideration of viscous effects and partial saturation.

3.1 Normal Consolidation and Critical State Line

As typically done with clays, this model distinguishes between normal consolidated sates and overconsolidated states. The first is identified at isotropic stress states

$q = 0$ when the void ratio is equal to $e = e_i$, whereby e_i is the maximum void ratio defined as:

$$e_i = e_{i0} - \lambda \log(p/p_{\text{ref}}) \tag{15}$$

where e_{i0} is a parameter describing the value of the maximum void ratio e_i at $p = p_{\text{ref}} = 1$ kPa, the scalar λ is the compression index and $p_{\text{ref}} = 1$ kPa is a reference (fixed) value. Notice that Eq. 15 is the relation originally proposed by the modified Cam-clay model. The Hvorlesv pressure $p = p_i$ is the maximum pressure at constant void ratio, which is obtained from Eq. 15:

$$p_i = \exp\left((e_{i0} - e)/\lambda\right) \tag{16}$$

The critical void ratio e_c follows also from the relations of the modified Cam-clay:

$$e_c = (e_{i0} - \lambda \log(2)) - \lambda \log(p/p_{\text{ref}}) \tag{17}$$

where $e_{c0} = e_{i0} - \lambda \log(2)$ is the critical void ratio at $p = 1$ kPa. The term $\lambda \log(2)$ in Eq. 17 comes from the fact, that once the critical state is reached, the mean pressure yields accordingly to a value of $p = p_i/2$.

Within the stress space, the model incorporates a bounding surface to describe some observations like the peak stress ratio of the material, and a critical state surface governing the behavior at large deformations ($|| \varepsilon || > 25\,\%$). Similar to the ISA model for sands by Fuentes [4] and some bounding surface models [1, 8], a "loading direction" tensor is introduced to project at these surfaces the current stress ratio $\mathbf{r} = \boldsymbol{\sigma}^*/p$, whereby $\boldsymbol{\sigma}^*$ is the deviator stress. The loading direction tensor is denoted by $\mathbf{n}$ and defined according to Fuentes [4]:

$$\mathbf{n} = \left[\overrightarrow{\mathbf{r}} + \langle -\overrightarrow{\mathbf{r}} : \mathbf{N}^* \rangle (\overrightarrow{\mathbf{N}^*} - \overrightarrow{\mathbf{r}})\right]^{\rightarrow} \tag{18}$$

The critical state surface is described with the condition $F_c \equiv F_c(\boldsymbol{\sigma}, \mathbf{n}) = 0$, whereby:

$$\text{Critical state surface:} \qquad F_c \equiv \mathbf{r} : \mathbf{n} - r_c = 0, \qquad r_c = \sqrt{2/3} M_c g(\theta_{\mathbf{n}}) \tag{19}$$

where M_c is the critical state slope for triaxial compression in the $p - q$ space and the scalar function $g = g(\theta_{\mathbf{n}})$ is evaluated with the Lode's angle $\theta_{\mathbf{n}}$ of the loading direction tensor $\mathbf{n}$. This function is responsible of the shape of the critical state surface seen from a deviator plane, as schematically shown in Fig. 2. It ranges between $c \leq g \leq 1$ whereby $c = M_e/M_c = 3/(3 + M_c)$ represents the ratio between the critical state slope for triaxial extension M_e and triaxial compression M_c according to Mohr-Coulomb. The function defining g follows the simple relation:

$$g(\theta) = \frac{2c}{(1 + c) - (1 - c)\cos(3\theta)} \tag{20}$$

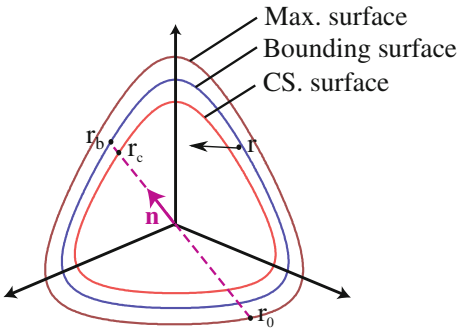

Fig. 2 Stress ratio images at the maximum surface, bounding surface, and critical state surface

The bounding surface represents the condition $\| \bar{\dot{\epsilon}}^p \| / \| \dot{\epsilon} \| = Y = 1$ within the stress space. According to Eq. 14, if the strain rate is in the same direction as the flow rule $\overrightarrow{\dot{\epsilon}} = \mathbf{m}$, the stresses would not change $\dot{\boldsymbol{\sigma}} = \mathbf{0}$ at the bounding surface. This is advantageous, because one may associate the shape of this surface as the maximum stress ratios $\| \mathbf{r} \|$ reached by the experiments. Within this model, the clay anisotropy due to the loading history is considered though the effect of the intergranular strain and not by the bounding surface. This means that, even this bounding surface does not present an additional rotational mechanism to simulate the clay anisotropy, such as in [2, 7], this latter effect is simulated through the small strain effects provided the intergranular strain formulation. The shape of the bounding surface is similar to [4], with a wedge-capped form (see Fig. 3):

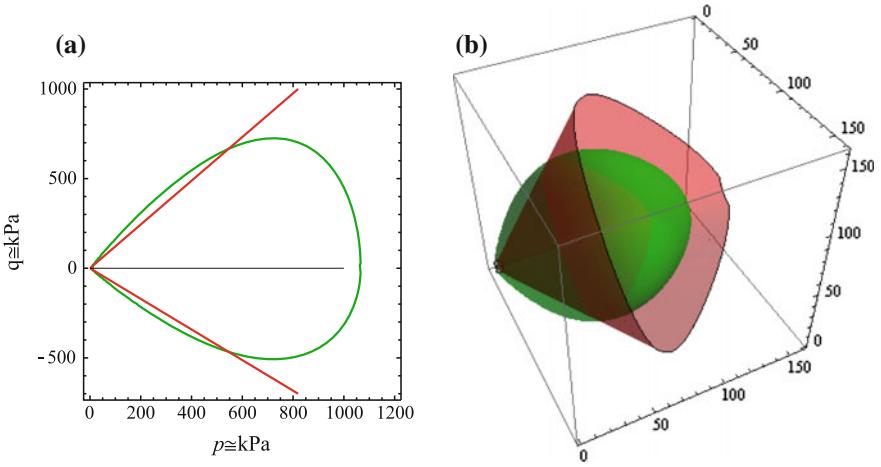

Fig. 3 **a** bounding surface within the $q - p$ space. **b** Bounding surface and critical state surface within the principal stress space

Bounding surface: $$F_b \equiv \mathbf{r} : \mathbf{n} - r_c f_b = 0 \quad \text{with} \quad f_b = f_{b0}\left(1 - \left(\frac{e}{e_i}\right)^{n_F}\right)^{1/2} \tag{21}$$

where $f_{b0} > 1$ is a material parameter defining the maximum norm of the stress ratio $\| \mathbf{r} \|$ at overconsolidated states and n_F is an exponent controlling the intersection of this surface with the critical state surface and defined as [4]:

$$n_F = \frac{\log\left((f_{b0}^2 - 1)/f_{b0}^2\right)}{\log(e_c/e_i)} \tag{22}$$

Notice that the fact that f_{b0} controls the norm of the maximum stress ratio allows to use this model for overconsolidated states. Hence, the surface described with:

$$\text{Maximum surface:} \qquad F_{b0} \equiv \mathbf{r} : \mathbf{n} - r_c f_{b0} = 0, \tag{23}$$

is the one controlling the maximum stress ratio for all states independently of the void ratio. Figure 2 gives a schematic illustration of this surface.

3.2 Stiffness Tensor

The residual stiffness $\bar{\mathsf{E}}$ is defined as in [4]:

$$\bar{\mathsf{E}} = 3\bar{K}\,\overrightarrow{\mathbf{1}}\,\overrightarrow{\mathbf{1}} + 2\bar{G}\left(\mathsf{I} - \overrightarrow{\mathbf{1}}\,\overrightarrow{\mathbf{1}}\right) - \frac{\bar{K}}{\sqrt{3}M_c}(\mathbf{1r} + \mathbf{r1}) \tag{24}$$

The bulk modulus $K = m\bar{K}$ and shear modulus $G = m\bar{G}$ are now adjusted to the behavior of clays with the following relations:

$$\bar{K} = \frac{K^L}{(1 - Y_{im})} = \frac{p}{\lambda_i}\frac{(1+e)}{(1 - Y_{im})} \tag{25}$$

$$\bar{G} = Kr \quad \text{with} \quad r = \frac{1 - 2\nu}{2(1+\nu)} \tag{26}$$

where ν is a material parameter (Poisson ratio) and the factor $Y_{im} = (r_K - 1)/(r_K + 1)$ depends on the function $r_K = \lambda/\kappa$, whereby κ is the swelling index considered as a material parameter. The details of the formulation of tensor $\bar{\mathsf{E}}$ can be found in [5, 10].

3.3 Residual Plastic Strain Rate $\bar{\dot{\epsilon}}^P$

The residual plastic strain rate tensor $\bar{\dot{\epsilon}}^P$ is proposed similar to some Karlsruhe hypoplastic models [10]:

$$\bar{\dot{\epsilon}}^P = Y\mathbf{m} \parallel \dot{\boldsymbol{\epsilon}} \parallel \tag{27}$$

whereby $Y = \parallel \bar{\dot{\epsilon}}^P \parallel / \parallel \dot{\boldsymbol{\epsilon}} \parallel$ is called the degree of nonlinearity [10] and $\mathbf{m}$ is the flow rule. This latter is defined identically as in Fuentes [4] but with a dilatancy surface equal to the critical state surface:

$$\mathbf{m} = \left(-1/2(r_c - \mathbf{r} : \mathbf{n})\mathbf{1} + \parallel \mathbf{N}^* \parallel \mathbf{n}\right)^{\rightarrow} \tag{28}$$

whereby $r_c = \sqrt{2/3}M_c g$ is the norm of the image stress ratio tensor at the critical state surface and the factor $g = g(\mathbf{n})$ has been previously defined in Eq. 20. The degree of nonlinearity Y is dictated by the relation according to [5]:

$$Y = \left(\frac{\parallel \mathbf{r} - \mathbf{r}_0 \parallel}{\parallel \mathbf{r}_b - \mathbf{r}_0 \parallel}\right)^{n_Y} \tag{29}$$

with the image stress ratio $\mathbf{r}_b = \sqrt{2/3}M_c g f_b \mathbf{n}$ and the image stress ratio at the maximum surface $\mathbf{r}_0 = \sqrt{2/3}M_c f_{b0}\mathbf{n}$, as depicted schematically in Fig. 2. As in Fuentes [4], the exponent n_Y controls the value of $Y = Y_i$ at isotropic states $q = 0$ through the relation:

$$n_Y = \frac{\log(Y_i)}{\log(f_{b0}/(f_{b0} + f_b/c))} \tag{30}$$

Whereby Y_i can be defined independently to simulate the behavior at isotropic states $q = 0$. Probably, the definition of Y_i is one of the key features of this model compared to the one for sands [4] because it now considers the effect of the overconsolidation. To do this, a factor $(p/p_i)^2$ is introduced to its definition as follows:

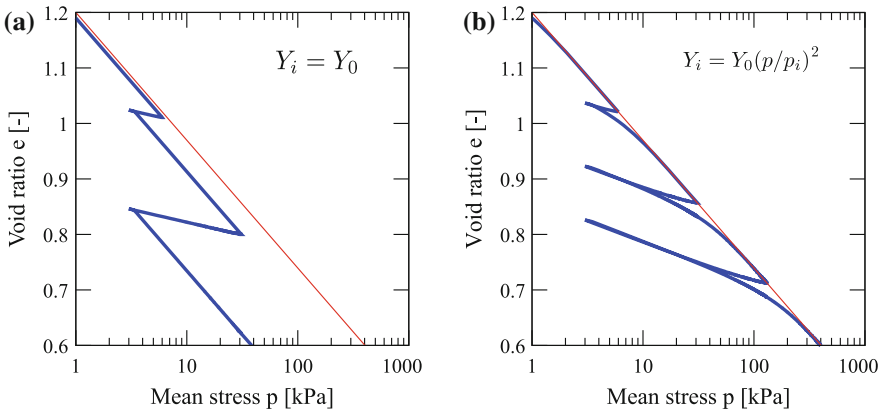

Fig. 4 Simulation of loading-unloading cycles at isotropic states $q = 0$ for different definitions of Y_i. **a** with $Y = Y_0$, **b** with $Y = Y_0(p/p_i)^2$

$$Y_i = Y_{im}(p/p_i)^2 = \left(\frac{r_K - 1}{r_K + 1}\right)(p/p_i)^2 \tag{31}$$

In order to show the influence of the factor $(p/p_i)^2$, some simulations at isotropic conditions $q = 0$ are provided in the Fig. 4. If this factor is not considered, the simulations shows ratcheting as in Fig. 4a. Simulations of the Fig. 4b shows an improvement avoiding this shortcoming.

4 Parameters and Numerical Implementation

The model requires 10 parameters listed within the Table 1. The Table presents also the description, units, approximated range, and some useful experiments for their calibration. These parameters include the basic parameters of the modified Cam-clay model namely λ, κ, e_0, ν, and M_c plus one parameter describing the maximum stress ratio f_{b0} at overconsolidated states and four additional parameters from the intergranular strain model m_R, R, β, χ_h. For their calibration, some routine tests are required, such as isotropic compression test, undrained triaxial test, drained triaxial test, and some cyclic tests.

The implementation has been performed by using a substepping explicit scheme with small strain subincrements to avoid numerical problems. The programming

Table 1 Material constants of the proposed model

Description		Units	Approx. range	Value	Useful experiments
Modified Cam-Clay					
λ	Compression index	(−)	10^{-6}−1	0.0057	IC$^{(i)}$
κ	Swelling index	(−)	10^{-6}−1	0.0057	IC$^{(i)}$
e_{i0}	Maximum void ratio	(−)	0.5−2	1.21	IC
ν	Poisson ratio	(−)	0−0.5	0.18	UTC$^{(ii)}$
M_c	CS slope	(−)	10−40	1.33	UTC, DTC
Hvorslev surface					
f_{b0}	Bounding surface factor	(−)	1−2	1.35	UTC, DTC
Intergranular strain					
m_R	Stiffness factor	(−)	1−7	5	CUTC$^{(iv)}$
R	IS yield surface radius	(−)	10^{-5}−10^{-4}	1.4×10^{-4}	–
β	IS hardening parameter	(−)	0−1	1.0	CUTC
χ_h	IS exponent	(−)	1−10	7	CUTC

(*i*) *IC* Isotropic test (loading-unloading)
(*ii*) *UTC* Undrained triaxial test
(*iii*) *DTC* Drained triaxial test
(*iv*) *CUTC* Cyclic undrained triaxial test

language corresponds to Fortran and follows the syntax of the subroutine UMAT from the software Abaqus Standard. The numerical integration of this subroutine has been performed with the software Incremental Driver which is fully compatible with the syntax of the UMAT subroutine.

5 Simulation Examples

This section presents some qualitative simulations with the proposed model. The parameters are typical for clay-like soils but has not been calibrated to any particular material. Hence, these simulations are qualitative to analyze the model response under some particular type of loading paths. For comparison purposes, some simulations with the modified Cam-clay model having the same counterpart parameters are presented. In all these simulations, the intergranular strain and back-intergranular strain where initialized with $\mathbf{h} = -R\mathbf{1}$ and $\mathbf{c} = -R/2\mathbf{1}$ to consider the effect of the initial isotropic compression before proceeding with the triaxial shearing.

Samples sheared under monotonic undrained loading were simulated and are shown in Fig. 5. Before the undrained shearing, all samples were isotropically compressed till $p = 200$ kPa reaching a void ratio of $e = 0.67$ and some of them were unloaded to different pressures. In this way, four different overconsolidated ratios OCR have been considered and correspond to OCR = {1, 2, 3, 4}. Simulations with the Modified Cam Clay model MCC have been included for comparison purposes, see Fig. 5a, c. The simulations with the MCC model show the well-known problems of this model when simulating heavy overconsolidated states (OCR $>$ 2), namely the overestimation of the peak stress ratio and the brittle transition from the elastic to plastic state. The ISA model does not present these disadvantages because the maximum stress ratio is controlled through the parameter f_{b0} and the transition from elastic to plastic states is very smoothed by the hardening of the IS yield surface.

The Fig. 6 presents the simulations of a cyclic undrained triaxial test with constant deviatoric stress amplitude and with 20 cycles. The cycles start at $p = 200$ kPa with a void ratio of $e = 0.67$. This illustrative example shows that under this cyclic loading path, the ISA model shows always plastic accumulation and finds an attractor (superimposed stress path cycles) when it reaches the critical state line, see Fig. 6b. Most of the experiments show that this attractor presents an "eight"-shape, but is attributed to the viscous effects in some plastic clays which has not been considered in the present formulation.

Figure 7 presents some simulations of cyclic undrained triaxial tests but now with constant strain amplitudes. Two simulations were included, the first with $|| \Delta\varepsilon || = 0.02$ and the second with $|| \Delta\varepsilon || = 0.005$. The cycles were performed after simulating a "large" cycle as shown in the figure. The simulations highlight the fact, that the "point attractor" (liquefaction) shape is achieved with the current model.

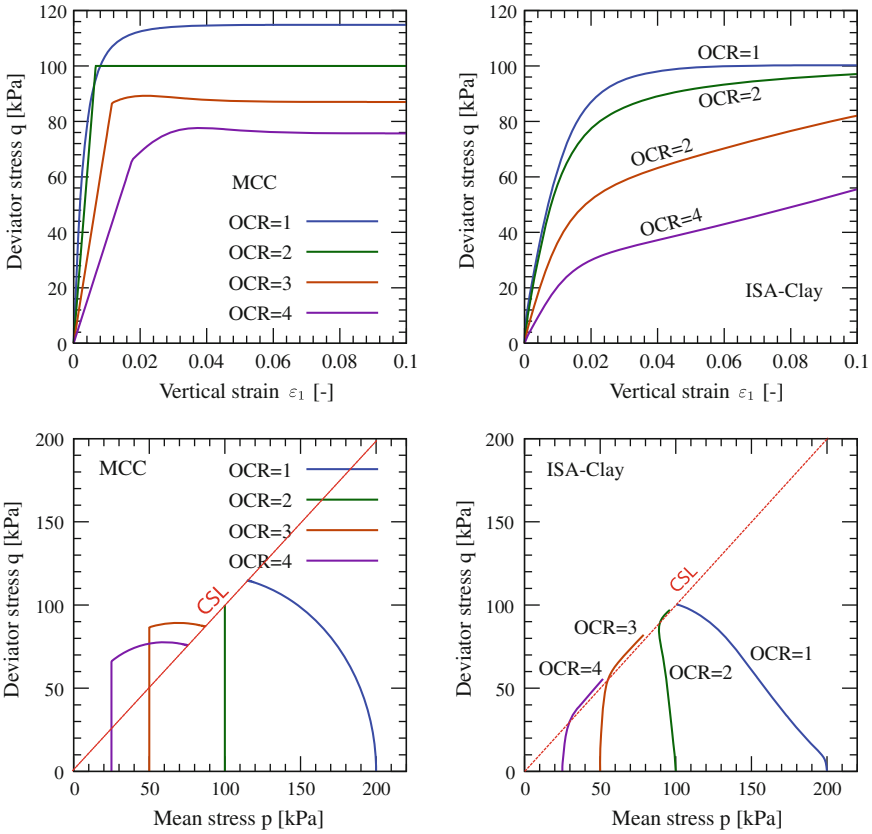

Fig. 5 Simulations of monotonic undrained triaxial test for different OCR. ISA model for clays (ISA-clay) is compared with the modified cam clay model (MCC)

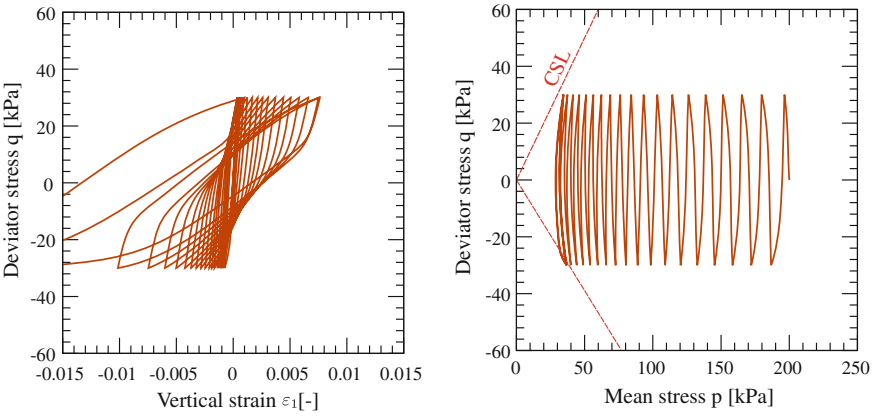

Fig. 6 Simulation with the ISA model for clays of a cyclic undrained triaxial test with constant deviator stress amplitude

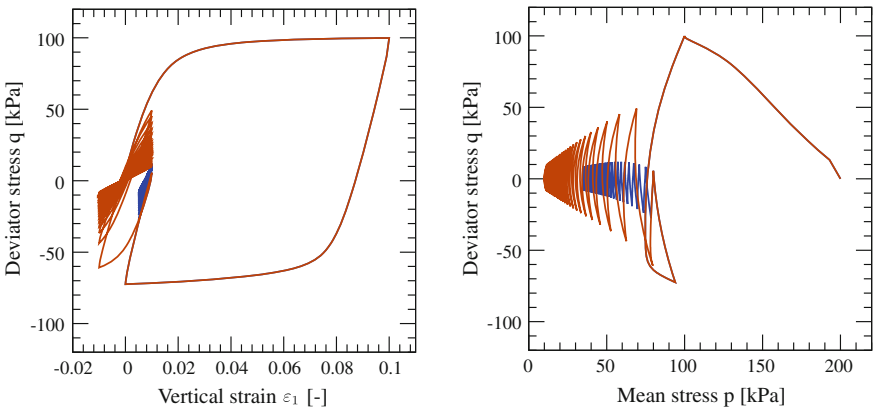

Fig. 7 Simulations with the ISA model for clays of a cyclic undrained triaxial test with constant strain amplitude (*blue* $|| \Delta\varepsilon || = 0.005$; *red* $|| \Delta\varepsilon || = 0.02$ and after a large cycle)

6 Closure and Outlook

In this article an ISA-type constitutive model for clays has been proposed. The model is based on the intergranular strain plasticity, which provides an alternative way to propose constitutive formulations describing the cyclic behavior of some soils. Similar relations as the ISA model for sands [4] were herein adopted and modified to simulate the clay behavior. The qualitative simulations showed that under some cyclic undrained loading paths, the attractors shown by the model are similar to those observed in many experiments. The next step, is to perform more validations through the simulation of experimental results and the incorporation of some effects as the material viscosity, partial saturation and cementation as well as the anisotropy.

References

1. Dafalias, Y.: Bounding surface plasticity. I: Mathematical foundation and hypoplasticity. J. Eng. Mech. ASCE **112**(9), 966–987 (1986)
2. Dafalias, Y., Manzari, M., Papadimitriou, A.: Saniclay: simple anisotropic clay plasticity model. Int. J. Num. Anal. Meth. Geomech. **30**, 1231–1257 (2006)
3. Fuentes, W.: Contributions in mechanical modelling of fill materials. PhD thesis, Karlsruhe Institute of Technology, KIT, Germany. Heft No. 179 (2014)
4. Fuentes, W., Triantafyllidis, T.: ISA model: a constitutive model for soils with yield surface in the intergranular strain space. Int. J. Num. Anal. Meth. Geomech. **39**, 1235–1254 (2015)
5. Fuentes, W., Triantafyllidis, T., Lizcano, A.: Hypoplastic model for sands with loading surface. Acta Geotech. **7**, 177–192 (2012)
6. Kolymbas, D.: Eine konstitutive Theorie für Boden und andere körnige Stoffe. Habilitation Thesis, Universität Karlsruhe, Germany. Institut für Boden- und Felsmechanik, Heft 109 (1988)
7. Leoni, M., Karstunen, M., Vermeer, P.: Anisotropic creep model for soft soils. Géotechnique **58**, 215–226 (2008)

8. Manzari, M., Dafalias, Y.: A critical state two-surface plasticity model for sands. Géotechnique **47**(2), 255–272 (1997)
9. Masin, D.: A hypoplastic constitutive model for clays. Int. J. Numer. Anal. Meth. Geomech. **29**(4), 311–336 (2005)
10. Niemunis, A.: Extended hypoplastic models for soils. Habilitation, Schriftenreihe des Institutes für Grundbau und Bodenmechanil der Ruhr-Universität Bochum, Germany. Heft 34 (2003)
11. Niemunis, A., Herle, I.: Hypoplastic model for cohesionless soils with elastic strain range. Mech. Cohesive-Frictional Mater. **2**, 279–299 (1997)
12. Niemunis, A., Prada-Sarmiento, L., Grandas-Tavera, C.: Paraelasticity. Acta Geotech. **6**, 1–14 (2011)
13. Wolffersdorff, V.: A hypoplastic relation for granular materials with a predefined limit state surface. Mech. Cohesive Frictional Mater. **1**, 251–271 (1996)